



## Article

# Damage States Investigation of Infilled Frame Structure Based on Meso Modeling Approach

Isyana Ratna Hapsari <sup>1,\*</sup>, Stefanus Adi Kristiawan <sup>2,\*</sup> , Senot Sangadji <sup>3</sup> and Buntara Sthenly Gan <sup>4</sup> <sup>1</sup> Civil Engineering Department, Sebelas Maret University, Surakarta 57126, Indonesia<sup>2</sup> SMARTCrete Research Group, Civil Engineering Department, Sebelas Maret University, Surakarta 57126, Indonesia<sup>3</sup> SMARTQuake Research Group, Civil Engineering Department, Sebelas Maret University, Surakarta 57126, Indonesia<sup>4</sup> Department of Architecture, College of Engineering, Nihon University, Koriyama 9638642, Japan

\* Correspondence: isyanahapsari@student.uns.ac.id (I.R.H.); s.a.kristiawan@ft.uns.ac.id (S.A.K.)

**Abstract:** The non-linear behavior of infilled frames is very complex. The behavior of this structure may be studied by experimental and numerical approaches. An experimental test can provide a more realistic output but has the disadvantages of high costs, relatively long time and specific room usage. A numerical analysis can be an alternative to analyze the behavior of infilled frames. One of the most powerful numerical approaches is meso-modeling. This approach has the advantage of being able to capture local damage to the panel. For this reason, the progressive damage identified in the meso-model can be used as a basis for determining damage state criteria. The grouping of damage states is proposed based on the initial identification in the form of local damage linked to global damage, i.e., IDR. This study's proposed level of infilled frame damage is DS1 = 0.17%, DS2 = 0.52%, DS3 = 0.79% and DS4 = 1.99%. However, the quantification results of the structural damage level cannot be generalized because many complex factors influence the behavior of infilled frames. Subsequently, a parametric study was carried out to determine the contribution of the mechanical properties of the infilled frame material to the degree of structural damage.

**Keywords:** numerical model; infilled frame; meso-modeling; damage states; local damage



**Citation:** Hapsari, I.R.; Kristiawan, S.A.; Sangadji, S.; Gan, B.S. Damage States Investigation of Infilled Frame Structure Based on Meso Modeling Approach. *Buildings* **2023**, *13*, 298. <https://doi.org/10.3390/buildings13020298>

Academic Editor: Bartolomeo Pantò

Received: 29 November 2022

Revised: 7 January 2023

Accepted: 14 January 2023

Published: 19 January 2023



**Copyright:** © 2023 by the authors. Licensee MDPI, Basel, Switzerland. This article is an open access article distributed under the terms and conditions of the Creative Commons Attribution (CC BY) license (<https://creativecommons.org/licenses/by/4.0/>).

## 1. Introduction

Buildings with infill walls with concrete or steel frames are commonly used in construction in various countries, especially for residential homes. The majority of structural analysis considers infill walls only as non-structural elements without contributing to the strength and stiffness of the structure. This is due to the many uncertain variables that affect the behavior of infill wall panels. In addition, there were some difficulties in modeling infills with various typologies [1]. However, many studies have been carried out and have demonstrated the contribution of the infills to the overall strength and stiffness of the frame structure [2–5]. The infill walls can contribute beneficially or detrimentally to the behavior of the structure [6–8], depending on various factors, such as the relationship between the frame and the wall, the strength and stiffness of the frame and the wall, as well as the mechanical properties of the structural materials [9].

The uncertain response of infilled wall structures occurs due to the complexity of factors [10]. This is because the infilled frame is a composite structure consisting of concrete, steel, mortar and bricks; all of these materials have different properties. In addition to these factors, the configuration of vertical loads, reinforcement ratios and geometric factors of infill structures also add to the complexity of the behavior of infill frames [11]. Several geometric factors of infilled wall structures include the percentage of wall openings, location of openings in walls, number of stories, structural dimensions, construction techniques and others. It is these various kinds of uncertainty variables that cause the behavior of

structures to become very complex and non-linear [12]. Therefore, a comprehensive infilled wall structure study is needed in the form of an appropriate and reliable model approach to obtain a structural response close to actual conditions.

The seismic response of structures can be analyzed using an experimental approach using full-scale tests. Several experimental studies have been carried out with various loading conditions (e.g., table shaking, cyclic and quasi-static, etc.) and different parameters (e.g., reinforcement effect, multiple column effect, etc.) to understand the behavior of infilled frames [13–15]. This methodology can obtain structural behavior similar to the existing structure. However, it also has the disadvantage of being high-cost and time-consuming while also requiring a specific place and adequate testing equipment [16–18]. On the other hand, numerical analysis is useful because it does not require a particular place, the cost is relatively cheap and the time required is quite short without compromising the accuracy of the analysis results [19]. Many studies and research have been carried out related to the mechanism of modeling infilled wall structures in recent decades. Modeling techniques capable of simulating the behavior of infill structures are divided into three categories, i.e., micro modeling, meso modeling and macro modeling [20–22]. Making the model can be assisted using commercially available software with the model simplification method [23].

One method of determining damage states is an analytical approach. The analytical approach evaluates the structural vulnerability using the mechanical properties of certain structural parameters, for example, inter-story drift (IDR). IDR-based damage states are a design of simplification. In reality, the level of damage is influenced by many parameters, such as structural systems, construction materials, accumulation and distribution of structural damage, element failure modes, number of cycles, duration and acceleration of earthquakes [24]. Of course, this method has the advantage of being able to provide a quick solution in knowing the vulnerability value of a structure. On the other hand, some researchers have suggested that the evaluation of seismic performance for infilled structures requires consideration of the quantification of damage to non-structural components [8,9,25]. The values of DS have been proposed by several researchers based on the degree and severity of the crack pattern on the panel, as well as the failure typology of the brick units [26–28]. In addition, DS-based quantification of peak load achievement and strength reduction ratio achievement was also presented by Cardone et al. [27]. Considering time, place and cost, the seismic performance assessment of the structure can use an alternative, a validated numerical model. Progressive damage identified in the numerical model will be used to determine damage state criteria at various levels. The purpose of this mechanism is the ability to quickly identify structural performance through an assessment of structural damage, both local and global damage.

This paper investigates the behavior of infilled wall structures via a meso modeling approach to identify the structure's progressive local damage. Subsequently, the paper proposes a grouping of infilled frame damage states based on the local damage level related to global engineering parameters, i.e., inter-story drift ratio (IDR). Furthermore, this paper also conveys the relationship between the mechanical properties of structural materials and the degree of damage that occurs.

## 2. Various Approaches to Model an Infilled Frame

The classification and illustration of the different infilled frame modeling techniques can be seen in Figure 1. The three infilled frame modeling strategies can be explained as follows:

(a) *Micro Modeling*

Micro modeling is a method of discretizing structural elements, i.e., by dividing the structure into many elements to account for the local effects in very detailed portions [12]. The approach of this model is to make the bricks, mortar and brick–mortar interfaces, or together with the frame, into a different continuum element [29]. It aims to consider the effect of mortar joints with several criteria for the resulting joint failure. The benefits of micro modeling are that it can provide an overview of the behavior of the infilled frame structure; local effects related to cracks in each part of walls, beams and columns; the failure mode of the panel; and contact area failures.

(b) *Meso Modeling*

Despite its advantages, the downside of using the micro modeling is in the analysis phase of large-scale infilled wall structures. The micro modeling has negative consequences, i.e., greater computational effort and longer time in completing the analysis stages. For this reason, researchers try to find a way to model a reasonable large-scale infilled frame but with a much more concise computational effort called meso modeling. For meso modeling, the approach taken is almost the same as for micro modeling. The difference is that the bricks are modeled as a continuum element, but the mortar and mortar–brick joints are modeled together into one interface element. This method was first proposed by Page [30].

(c) *Macro Modeling*

This modeling method defines masonry units, mortar joints and unit–mortar interface joints as a single-element model of a homogeneous anisotropic continuum. The diagonal strut model is widely used and accepted as one of the best approach methods, simple but rational in describing the behavior of infilled structures. In this macro modeling, the infill wall panels are simulated using diagonal struts along the loading direction. The concept of wall modeling applying a macro approach model using diagonal supports was first proposed by Polyakov [31] and then underwent many transformations. Development using a single strut approach started from what was done by Crisafulli and Carr [32]. This method has advantages in the simplicity of mathematical formulas and has provided reasonable estimates in calculating the stiffness value. However, on the other hand, this method has the disadvantage of being unable to predict the shape of the deflection that occurs in the column and then produces shallow bending moment and shear force values [32,33]. Meanwhile, Kumar [34], El-Dakhkhni [35], Tanganelli [36] and Pashaie [37] argue that multi-struts modeling can produce the closest bending moment values when validated using a numerical model using FEM Software.

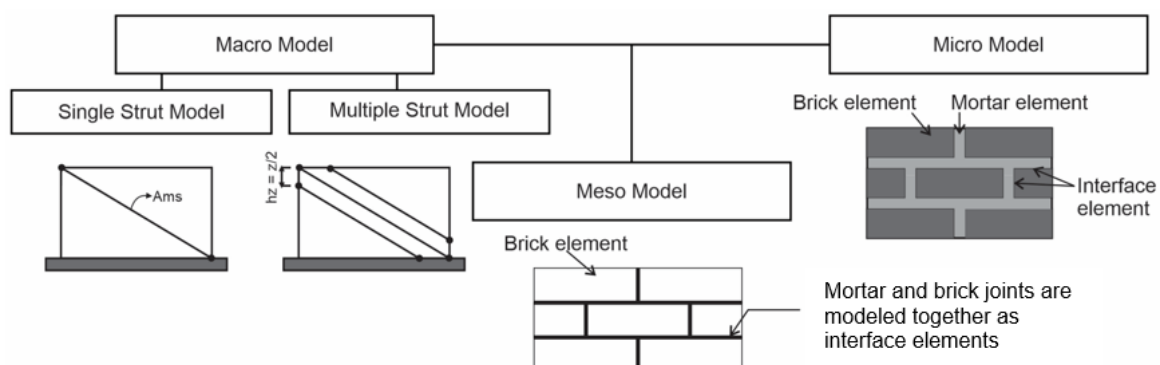


Figure 1. Developed infill frame modeling technique [12,20–22].

### 3. Damage States Definition

Several parameters are used to limit the structure's performance level, such as the value of stress, strain, maximum load, inter-story drift, acceleration between floors and physical damage that occurs. Some codes apply and state the concept of determining different levels of performance [38–40]. In addition, previous studies state that the damage

to panels for infilled frame structures is divided into 3 to 4 levels [26–28,40–42]. Based on the experimental result, some researchers propose different structural damage limits using IDR.

Analysis of structural performance in terms of inter-story drift value (IDR) is one of the most common simplification methods. A single design parameter such as drift value (IDR) alone may not adequately control all performance objectives of structural and non-structural systems [43]. Structural response, i.e., drift value (IDR), can be associated with macroscopic damage indicators in the form of crack severity values and failure of brick units. This response is then associated with the level of structural damage. Several researchers suggested the level of damage to the infilled frame in the form of IDR based on the test results. Researchers tried to connect the mechanical properties in the panel with the IDR to facilitate people to take practical and appropriate corrective actions in the design step.

According to Chiozzi [28], the classification of damage states for infilled frames by calculating the width of the cracks is then associated with the proposed appropriate IDR threshold. Zhang [44] proposes that the IDR limit is related to the shape and characteristics of the infill wall damage and refers to the existing performance index. A study conducted by Chun Hui Liu [41] classified the damage states of the infilled frame by considering the description of the damage and mechanical properties of infill walls. This damage description is based on the degree of cracking, block and mortar damage, loads in a plane and displacement. The database of Chun Hui Liu uses 132 infilled frame experiments from previous researchers. Cardone [27] said that observations on the severity of cracks, failure of brick units and damage to frames determined the damage states for infilled frames. Kalman Sipos [42] collects various infilled frame tests and makes averages of the drift value (IDR) that occurs at the first yield (IDR<sub>y</sub>) and ultimate point (IDR<sub>u</sub>). IDR<sub>y</sub> is the first point marked by a sudden decrease in the stiffness of the infilled frame. Meanwhile, IDR<sub>u</sub> is the ultimate point associated with the maximum lateral capacity. Table 1 summarizes some of this study's results and a code that quantifies damage states for infilled frames based on IDR, structural stiffness conditions, crack severity and the definition of wall panel damage states.

**Table 1.** The damage states the definition of infilled frame in some researchers and code.

Performance Level	Research Results & Codes				
	Cardone [27]	Chun Hui Liu [41]	Chiozzi [28]	Kalman Sipos [42]	FEMA273 [40]
DS1	Light diagonal crack, crack width < 1 mm, IDR = 0.06–0.46%	No crack, IDR = 0.1%	Crack width < 2 mm, IDR = 0.125%	First yield, IDR < 0.1%	IDR < 0.1%
DS2	The crack becomes wider 1–2 mm, cross-crack, IDR = 0.21–1.38%	A diagonal crack on the panel and different cracks start to connect, IDR = 0.3%	Crack width 2–4 mm, IDR = 0.327%	$0.1 \leq \text{IDR} < 0.3\%$	$0.1 \leq \text{IDR} < 0.3\%$
DS3	Crack width > 2 mm, starting to fail, IDR = 0.5–1.98%	Crack develops into a cross-crack, peak load, IDR = 0.9%	Crack width > 4 mm, IDR = 0.82%	Ultimate point, $0.3 \leq \text{IDR} < 0.75\%$	$0.3 \leq \text{IDR} < 0.6\%$
DS4	Failed/collapse, IDR = 1.06–3.26%	Collapse, IDR = 1.9%	-	$\text{IDR} \geq 0.75\%$	$\text{IDR} \geq 0.6\%$

## 4. Numerical Modeling Methods

### 4.1. Modeling Configuration

In this study, the modeling of the infilled frame structure uses a meso-model approach assisted by finite element software—ATENA 3D. The results of this numerical model

will later be validated using the results of the Kakaletsis experiment [45]. The scope of the analysis in this study will be focused on the full-infilled frame model resulting from the Kakaletsis test. One of this study's objectives is to see an effective and accurate numerical model approach when analyzing the behavior of infilled structures against the test results. In addition, from this meso model, the stages of quantifying damage states can be carried out by using output in the form of global and local parameters. Figure 2 gives a detailed description of the prototype of the building model. The portal structure uses gross height = 1500 mm and gross width = 1300 mm, with beam cross-sectional dimensions =  $100 \times 200$  mm and column cross-sections =  $150 \times 150$  mm. The dimension of the bricks is  $60 \times 60 \times 93$  mm. According to Kakaletsis, this portal model represents 1/3 scale of the prototype structure.

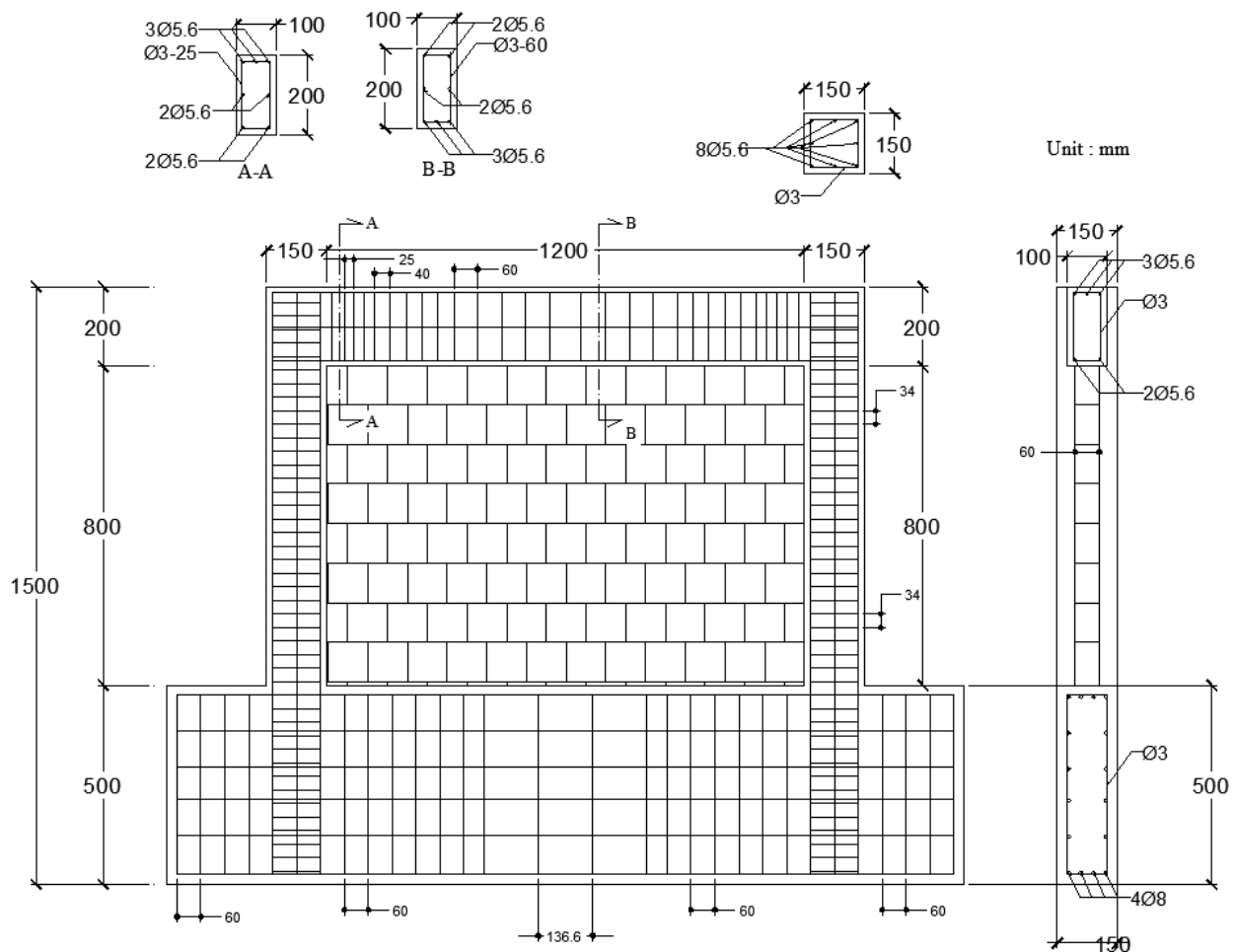


**Figure 2.** Construction details of the infilled frame specimen used in Kakaletsis experimental test.

#### 4.2. Meso Modeling Approaches

A finite element method is powerful when assessing structures' behavior due to earthquake loads [46]. The model is generally built from several macro elements that describe one or more parts of the test model specimen. In this study, infilled frame structure modeling uses ATENA 3D. Figure 3 provides information about the technique of detailing the parts of the meso modeling, divided into several macro elements, and the connection relationships between macro elements in one infilled frame structural system. Special attention for this meso modeling technique is making each brick unit by directly including the joint variable. The mortar joints between the bricks and frames, and between the bricks with adjacent bricks are simulated as a 3D gap connection (without thickness). The picture also shows that the steel plate is installed to transfer the load to the frame to avoid

numerical singularities caused by stress concentration, as for the relationship between the reinforcement and the frame using a perfect connection. Details on defining macro element meso modeling are generally presented in Table 2.

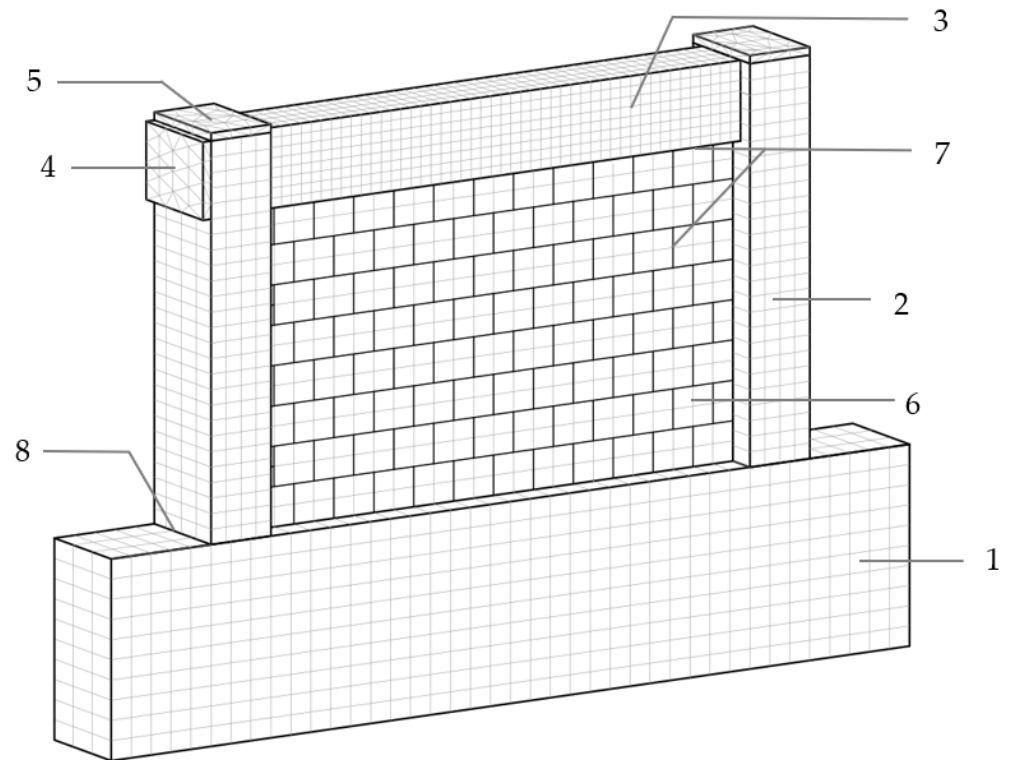


**Figure 3.** Macro elements, interfaces and meshing method of the meso model.

**Table 2.** General definition of macro element—the interface of meso modeling.

No	Name of Macro Element	Material Usage
1	Plinth beam (foundation)	Concrete
2	Column	Concrete
3	Beam	Concrete
4	Plate	Steel
5	Plate	Steel
6	Bricks	Masonry
7	Brick–Interface	3D Gap Connection
8	Macro element–Interface	Perfect Connection

The technique of dividing the mesh size within a structural element is essential for the quality of the numerical results. For fine meshing division with mesh size = 1/10 of the smallest structural element, it will cause longer computation time. Meanwhile, the results are less accurate for coarser meshing with a meshing size = 1/2 of the smallest structural element. The ideal mesh size uses a one-fourth value per each dimension of the structural element [47]. Based on this theory, the meshing size in each beam, column, sloof and wall element is different. In Figure 3 and Table 3, information is presented regarding the meshing configuration used in this modeling. In this study, the mesh size has used the most optimal size. Stages of sensitivity analysis to variations in mesh size have been carried out to obtain convergent mathematical calculations.

**Table 3.** Meshing configuration of meso modeling.

Element	Meshing Size (m)	Meshing Type
Plinth beam (foundation)	0.05	Brick
Column	0.0375	Brick
Beam	0.025	Brick
Plate	0.05	Tetra
Masonry	0.05	Brick

In ATENA 3D, the behavior of concrete as a frame is simulated using 3D NonLinear Cementitious 2. This type of material is also used for infill walls. This model combines constitutive models for tensile such as fracture and compressive–plastic behavior. The material model is based on orthotropic smeared crack formulation and the crack band model. This model uses Rankine failure criteria and uses exponential softening with rotated or fixed crack models. The hardening/softening plasticity model is based on the Menetrey–Willam failure surface [48]. A summary of initial parameter values for concrete, reinforcement and wall materials is based on the Kakaletsis test results [45]. The value of the tensile strength of concrete and brick walls ( $f_t$ ) is calculated using the Formula (1) [49]. Meanwhile, the  $E_c$  value, the elastic modulus of concrete, is calculated using the Formula (2) [50]. The specific fracture energy ( $G_f$ ) using the Equation (3) [47]. The material properties values for constructing an infilled frame model based on 3D finite elements are presented in Table 4.

$$f_t = 0.44 \sqrt{f_c'} \quad (1)$$

$$E_c = 4700 \sqrt{f_c'} \quad (2)$$

$$G_f = 0.0000025 f_t \quad (3)$$

The 3D interface material is based on the Mohr–Coulomb criterion without tension. This joint model defines two stiffness values, i.e., tangential stiffness ( $K_{tt}$ ) and normal stiffness ( $K_{nn}$ ). The numerical formula that Cervenka recommends for calculating the two stiffness values is as in Equations (4) and (5).  $E_i(\min)$  and  $G_i(\min)$  are the minimum value of the material's elastic modulus and shear modulus around the contact area per connected element;  $t$  is the thickness of the contact area. Values related to interface material properties are summarized in Table 5.

$$K_{nn} = \frac{\min\{E_i\}}{t} \quad (4)$$

$$K_{tt} = \frac{\min\{G_i\}}{t} \quad (5)$$

**Table 4.** Initial properties of the fracture–plastic constitutive model.

Description	Symbol	Concrete	Masonry	Unit	Ref
Elastic modulus	$E$	$2.510 \times 10^4$	$6.607 \times 10^2$	MPa	[45]
Poisson's ratio	$\mu$	0.200	0.100	/	
Tensile strength	$f_t$	2.349	0.260	MPa	
Compressive strength	$f_c$	$-2.851 \times 10^1$	-2.630	MPa	[45]
Specific fracture energy Equation (3)	$G_f$	$5.000 \times 10^{-6}$	$4.500 \times 10^{-1}$	N/mm	[47]
Crack spacing	$S_{max}$	0.125	/	m	
Tensile stiffening	$Ct_s$	0.400	/	/	[47]
Critical compressive disp.	$\omega_d$	$-5.000 \times 10^{-4}$	$-5.000 \times 10^{-4}$	/	[47,51,52]
Plastic strain at $f_c$	$\varepsilon_{cp}$	$-1.417 \times 10^{-2}$	$-1.358 \times 10^{-3}$	/	
Reduction of $f_c$ due to cracks	$r_{c,lim}$	0.800	0.800	/	[47]
Crack shear stiffness factor	$S_F$	$2.000 \times 10^1$	$2.000 \times 10^1$	/	
Aggregate size		$1.600 \times 10^{-2}$	/	m	
Fixed crack model coefficient		1.000	1.000	/	

**Table 5.** Initial interface material properties.

Description	Symbol	Value	Unit
Normal stiffness (Equation (4))	$K_{nn}$	$6.607 \times 10^4$	MPa
Tangential (shear) stiffness (Equation (5))	$K_{tt}$	$3.003 \times 10^4$	MPa
Tensile strength	$f_t$	0.420	MPa
Cohesion	C	0.520	MPa
Friction coefficient	$\Phi$	0.770	/

Reinforcement modeling using CCRinforcement type in the ATENA. Multilinear law with yield value ( $F_y$ ) and ultimate value ( $F_u$ ) of reinforcement uses Kakaletsis test results. Whereas the steel plate uses a homogeneous elastic model of 3D Elastic Isotropic type with the elastic modulus  $E = 200,000$  Mpa and Poisson's Ratio = 0.3.

Boundary conditions are such to replicate the test setup of Kakaletsis. This boundary condition is applied to a numerical model made to replicate the setting of the test object in the experiment. The boundary condition for infilled frame modeling is presented in Figure 4. The sloof beam is modeled as a clamp that is constrained in the Y and Z directions (point 1). The axial load of 50 kN is applied in each column (point 2a). Kakaletsis's experiment uses cyclic loading that applies a gradual increase in displacement control. This loading protocol uses seven amplitude sets. In one set of amplitudes, there are two cyclic loadings. The cycle starts from a ductility level of 0.8 or equal to an amplitude of about  $\pm 2$  mm. Then continue to increase gradually until the level of ductility 2, 4, 6, 8, 10 and 12, or according to the displacement of 6, 12, 18, 24, 30 and 36 mm. Whereas in this numerical model, the lateral load is applied gradually with displacement control as a quasi-static loading. The monitoring point is set as prescribed deformation in the lateral direction (point 2b). This homogeneous steel plate is installed as a load transfer plate to the structural elements, both lateral and axial loads (point 3). Based on the Kakaletsis experimental setting, the condition of the support structure should be rigid but still shows the possibility of deflection due to applied loading. Whereas for the X direction, it is free but given displacement constraints by the surface spring material, which is modeled as a CCSpring material, an elastic type material with an initial stiffness ( $K$ ) = 35 MPa (point 4).



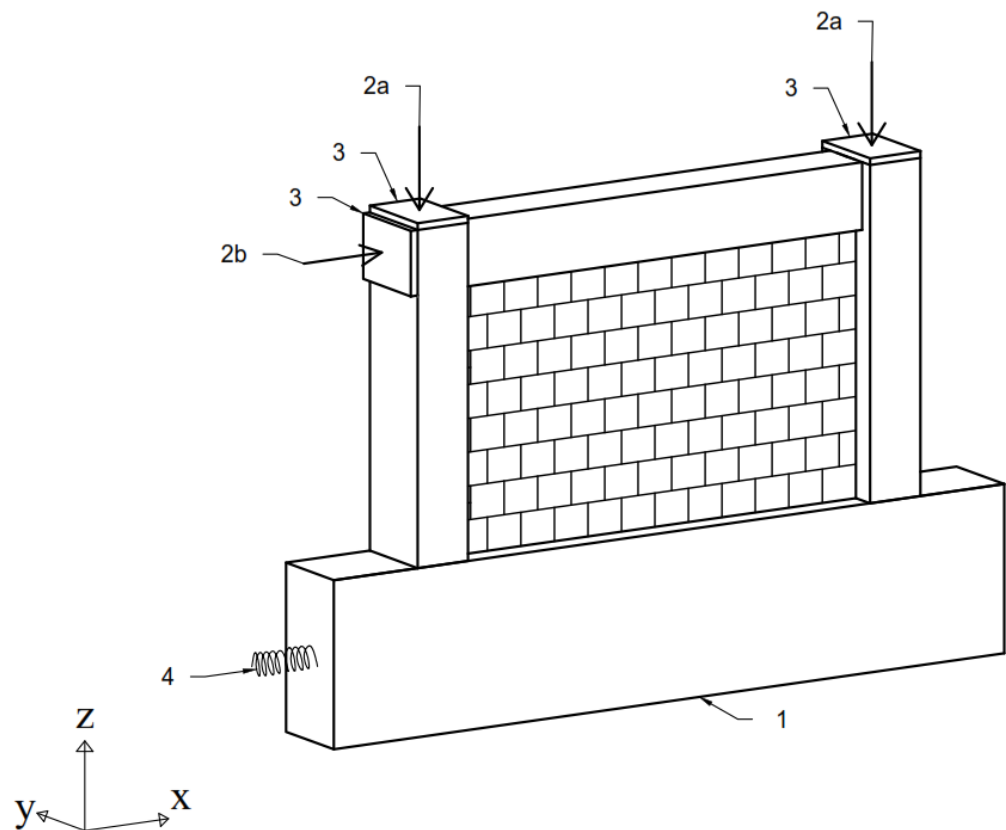


Figure 4. Boundary condition of meso-model-ATENA 3D.

## 5. Numerical Modeling Validation

The validation step starts from a bare frame. This validation stage is carried out using the capacity curve of the cyclic curve conversion of the Kakaletsis test results by connecting the outermost values (envelope). The results of the validation of the response of the structure are shown in Figure 5. The graph shows the similarity between the open-frame numerical model compared to the test. The conformance is quantified into validation on four (4) parameters, i.e., the displacement value at peak load, peak load, initial stiffness and residual strength at collapse. For initial stiffness obtained using Formula (6),  $F_y$  is yielding load, and  $\delta_y$  is yielding drift. The four parameters of this calibration benchmark show the average similarity at a value = 103%. Table 6 shows the comparative error value between the meso model and the experiment in detail. Because the capacity curve validation results show similarities, this open frame model can be used as a control model to proceed to infilled frame modeling.

$$K = \frac{F_y}{\delta_y} \quad (6)$$

After the open frame control model is obtained, the next stage is the infilled frame modeling. This stage is to add infill walls as structural elements. Infilled frame modeling uses the parameters given in Tables 4 and 5 and continues with the validation stage using the results of the Kakaletsis experiment. The results of the numerical modeling infilled frame response in this early stage can be seen in Figure 6. Nonlinear behavior due to the softening of masonry after the yield point and or the cracking of the panel modeled by a stiffness matrix that changes according to the degradation. This is also clarified by ATENA's theory, which states that the uncracked and cracked conditions have different stiffness matrices. The material stiffness matrix for the uncracked concrete has the form of an elastic matrix of the isotropic material. For the cracked concrete, the matrix has the form of the elastic matrix for the orthotropic material.

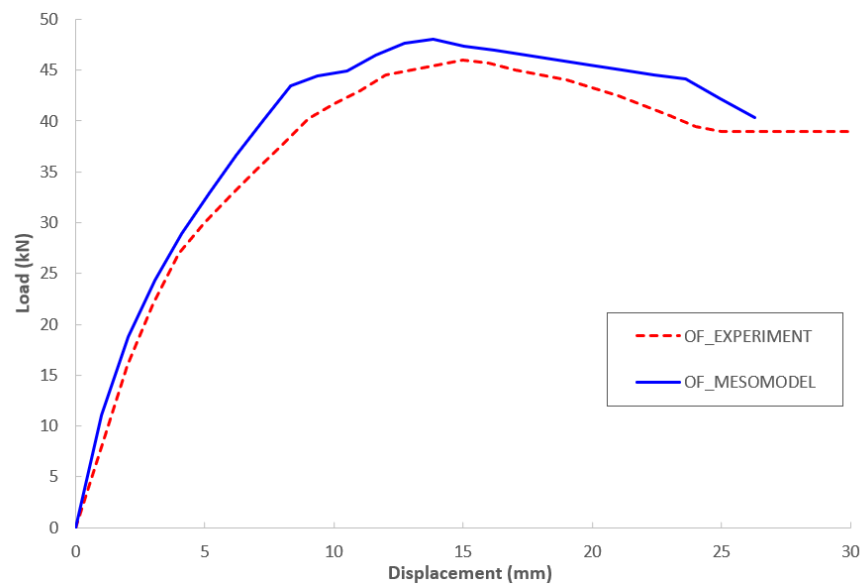


**Figure 5.** Capacity curve between open frame testing and meso modeling.

**Table 6.** Validation results for open frame meso model vs. experiment.

Parameters Quantification	Unit	Models		Similarity
		Experiment	Meso	
Peak load	kN	46.00	48.03	104%
Displacement at peak load	mm	15.00	13.83	92%
Initial stiffness	kN/mm	7.30	8.16	112%
Residual strength at the collapse	kN	39.00	40.31	103%

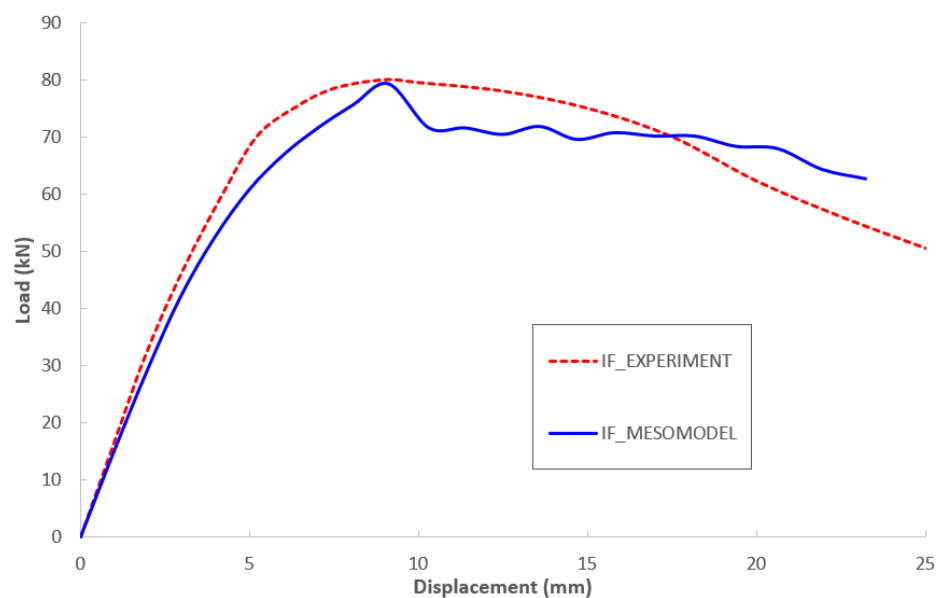


**Figure 6.** Capacity curve between infilled frame testing and meso modeling.

Through Figure 6, it can be seen that the value and position of the peak load, displacement at peak load, initial stiffness and residual strength show similarities of 99%, 101%, 87% and 115%, respectively. However, to improve the behavior of the after-peak load model, a sensitivity analysis is still carried out in the next stage. At this stage, the adjusted parameters are only the variables used to model the walls. The first adjustment stage is to vary the brick elastic modulus ( $E_m$ ) value. The initial value = 660 MPa, increased to 750 MPa and 900 MPa. The adjustment range for the modulus of elasticity of bricks is based on the results of research conducted by Crisafulli [1] that the value of  $E_m$  ranges from  $400 \text{ fcM} < E_m < 1000 \text{ fcM}$ . The resulting structural response when increasing the  $E_m$  value can be seen in Figure 7a. From the resulting graph, it can be seen that the greater the value of the modulus of elasticity of the brick, the higher the strength of the post-peak structure. This was done to get post-peak behavior close to the experiment.

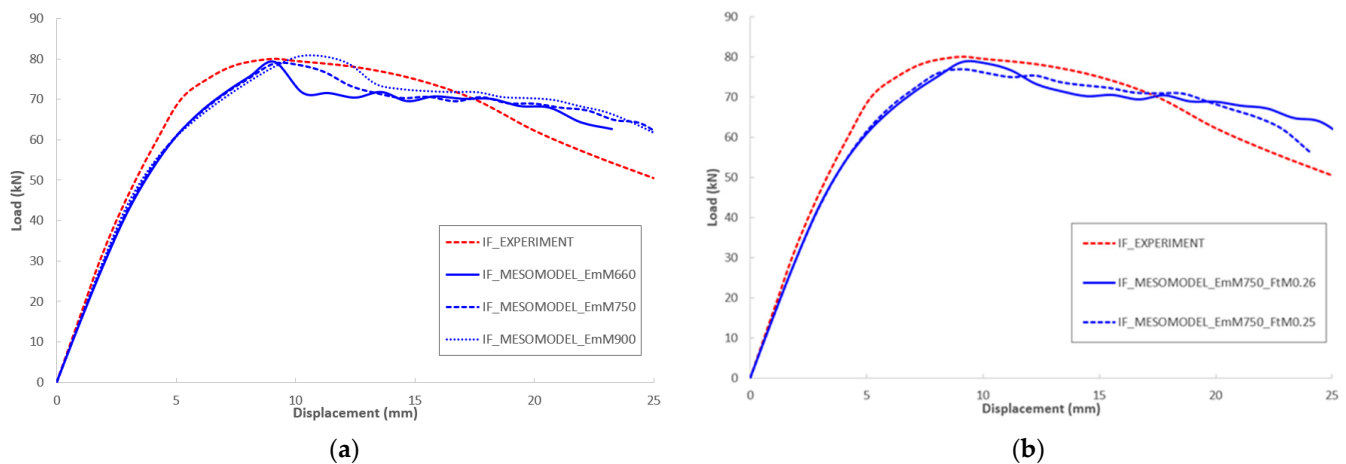


**Figure 7.** Example of infilled frame sensitivity analysis and validation result: (a) IF\_meso model with  $E_m$  variation; (b) IF\_meso model with  $f_t$  variation.

The load-deformation behavior of the infilled frame is influenced by material properties, including the elastic modulus of masonry ( $E_m$ ). For this reason, it is expected that the influence of  $E_m$  can be identified at the elastic phase as well. However, the structural condition of the support also significantly affects the behavior. In the experiment, the horizontal restraint was provided through anchorage to join the plinth beam and floor. Based on this experimental setting, the support condition still shows the possibility of lateral deformation due to applied loading. The numerical model adopted this by providing a horizontal elastic spring. Consequently, the load-deformation at the elastic phase is not sensitive to the  $E_m$  as that would occur in the case of a rigid connection.

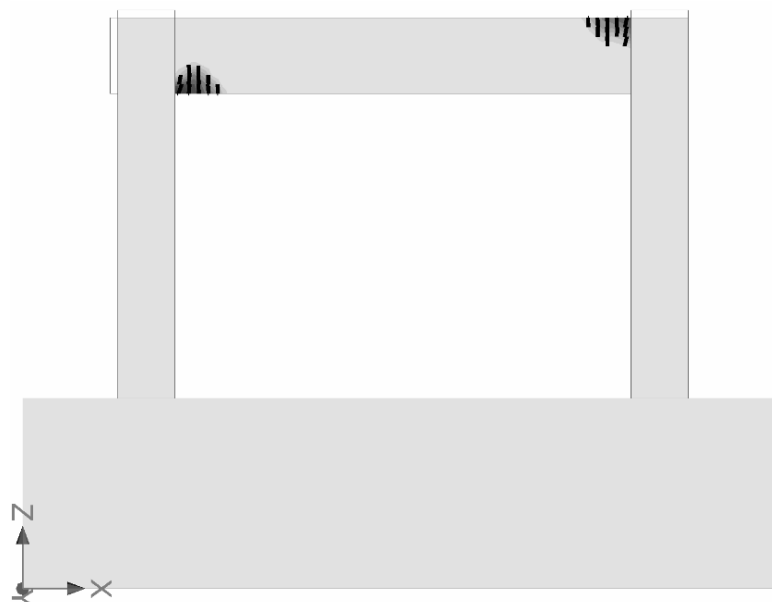
According to Lourenco [20], the tensile strength value of brick panels is 3–10% of the compressive strength value. Due to the slight difference in Figure 7a, a little adjustment is needed in the tensile strength of the bricks ( $f_t$ ), which was initially = 0.26 MPa to 0.25 MPa. According to studies conducted by previous researchers [53–55], this value is still in the range of brick tensile strength values of 0.16–0.58. The structural response generated using the  $f_t$  adjustment is shown in Figure 7b. From this figure, it can be seen that lowering the  $f_t$  value affects the decrease in the peak load value, increases the behavior of the after-peak load model and also reduces the residual strength. Therefore, the infilled frame model with a value of  $f_t = 0.25$  MPa can be used as an infilled frame model in the next analysis stage.

Based on the last model, i.e., IF\_MESOMODEL\_EmM750\_FtM0.25, the similarity of the calibration results with the experiment can be quantified in detail, as presented in Table 7.

**Table 7.** Validation results for infilled frame meso model vs experiment.

Parameters Quantification	Unit	Models		Similarity
		Experiment	Meso	
Peak load	kN	80.00	77.09	96%
Displacement at peak load	Mm	9.00	9.11	101%
Initial stiffness	kN/mm	16.67	14.80	89%
Residual strength at the collapse	kN	52.44	55.97	107%

The meso model can capture crack pattern information on open and infilled experimental frames. For the open frame meso model, the first crack occurs in the upper beam of the front of the column (Figure 8), and this also occurs in the experimental results presented by Kakaletsis. The meso model collapsed at IDR = 3.11%, almost similar to the experimental results, which informed that the test object collapsed at IDR = 2.80%. Figure 9a shows the mode of the meso crack pattern in the model and the test object—Figure 9b when the structure collapses.

**Figure 8.** The first crack that occurs in the meso-model.

The meso output of the infilled frame model is seen to have failed at IDR 1.99%, as shown in Figure 9c. Figure 9c shows a crack pattern mainly oriented from top left to bottom right, suggesting a diagonal strut orthogonally oriented. While the test results stated that the failure of the infilled wall structure occurred at IDR 1.9% with the mode of the crack pattern, as shown in Figure 9d. Figure 9d shows the failure mode composed of diagonal cracking and bed-joints sliding. The difference in the crack pattern from the numerical model with the experiment could be due to the type of connection adopted. In the numerical model, the connections between elements are not modeled in detail into separate macro elements but instead are modeled as interface elements although the properties of the interface element have tried to describe the actual mechanical properties of the mortar joints between the bricks. Apart from these factors, there are other factors, such as the loading protocol, used in the experiment using cyclic loading that applies a gradual increase in displacement control. Whereas in this numerical model, the lateral load is applied gradually with displacement control as a quasi-static loading.

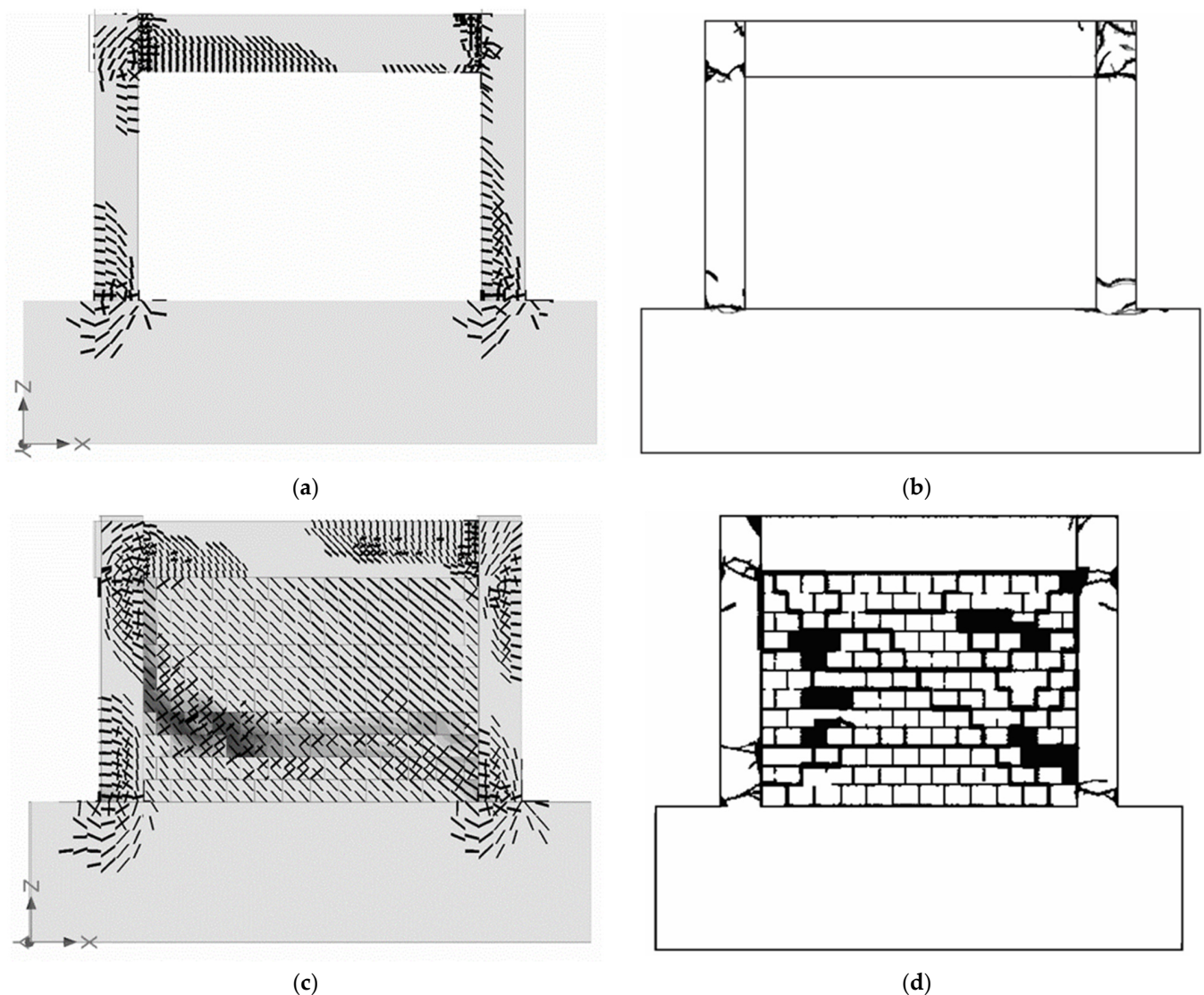


**Figure 9.** Comparison of failure mode: (a) Open Frame—meso model; (b) Open Frame—Kakaletsis's experiment; (c) Infilled Frame—meso model; (d) Infilled Frame—Kakaletsis's experiment.

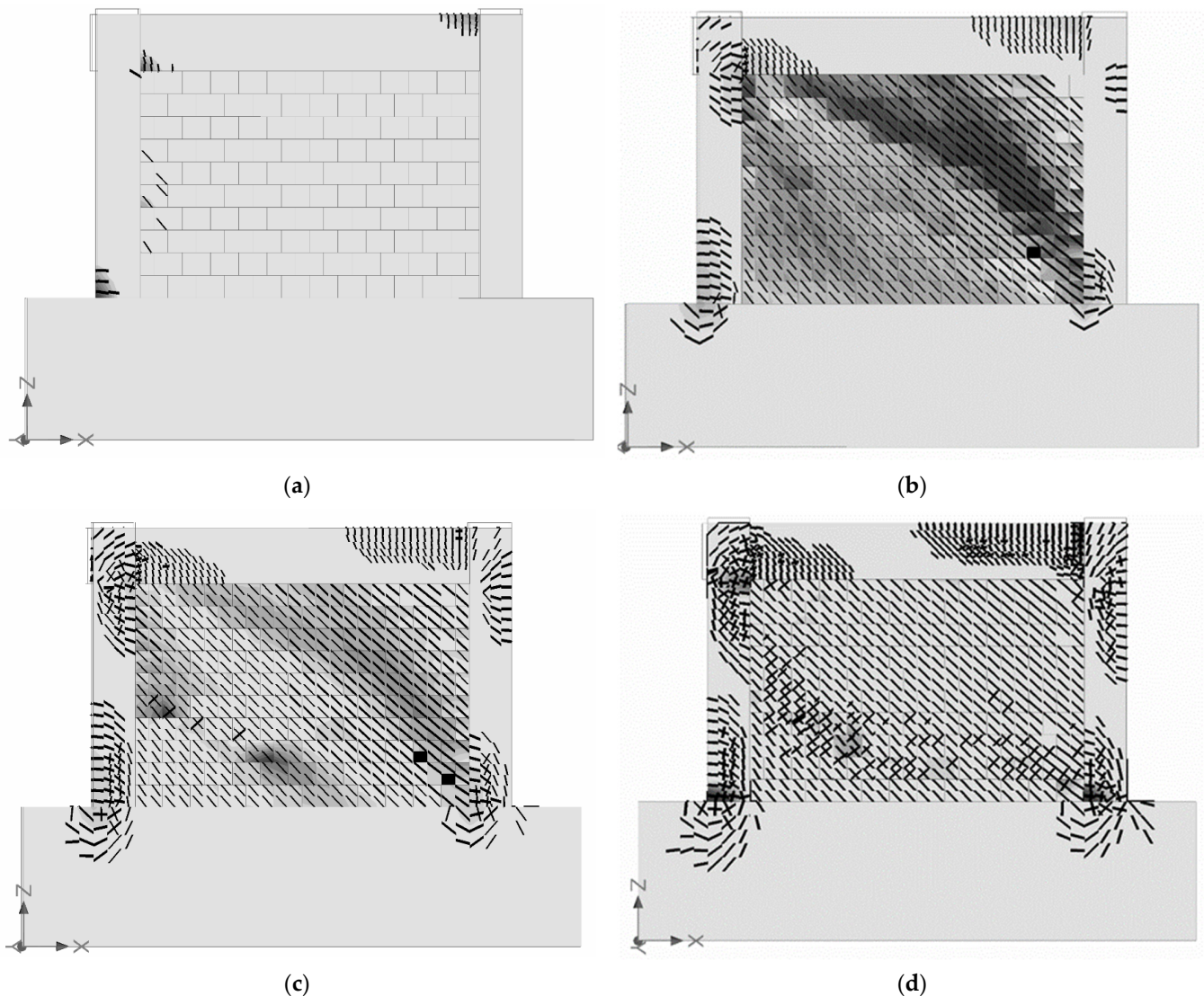
## 6. Damage States Analysis

From the structural response obtained from numerical modeling, some of the resulting values can be associated with structural performance limitations. The most commonly used value for quantifying structure level performance is the inter-story drift ratio (IDR). However, each inter-story drift (IDR) level will vary due to several factors, such as typologies, material properties, geometric factors and many more. For these reasons, for the more advanced, realistic and precise analysis, it is necessary to determine the damage limits of the infilled wall structure, i.e., IDR as a global behavior connected to local behavior such as crack width and failure mode.

The advantage of meso modeling is that local behavior values such as crack width and failure mode for both infill elements, beam, and column elements can be obtained through the output of the post-processor. In contrast, the weakness of macro modeling results is the inability to output local behavior values that occur in infilled panels. One of the things that cause macro modeling to be unable to capture local behavior is when the first initiate the diagonal strut model approach, i.e., by first predicting that the wall panel is damaged diagonally.

Determination of the damage limit based on the proposed IDR starts with quantifying the level of damage to the structure based on the mode of local damage to the panels,

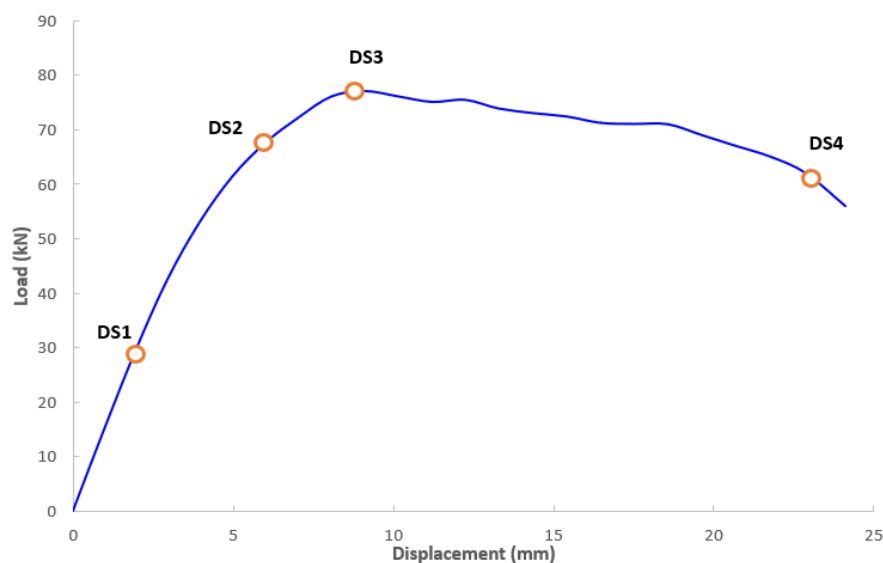
followed by the severity of the cracks. To obtain detailed information on the level of shape and severity of panel cracks, see Figure 10. The next step is measuring the crack width of the panel at each level of damage. After getting the level of damage based on local damage, it is then linked to global behavior. The global behavior assessment begins with the identification of the condition of the structure when it undergoes the elastic–plastic–ultimate–failed phase. At this stage, it is necessary to identify the degradation of stiffness values in each structural condition. After these stages are completed, it is continued by associating the IDR value with several levels of damage to the proposed structure. Of course, the drift values proposed as damage limits must be checked for compliance with applicable codes and previous research (Table 1). The definition of damage states is divided into 4 points, i.e., DS1 = slight damage, DS2 = moderate damage, DS3 = extensive damage and DS4 = near collapse. Through the data generated by the meso-model that has been validated by experiment, the proposed classification of damage states for infilled frames is presented in Table 8. A macro overview of damage points plotted on the capacity curve of infilled frames can be seen in Figure 11.



**Figure 10.** Proposed damage states of the infilled frame (failure mode and crack severity) based on meso model: (a) DS1; (b) DS2; (c) DS3; (d) DS4.

**Table 8.** Proposed Definition of Damage States for Infilled Frame based on Meso Model.

Performance Level	Proposed				
	Panel Failure Definition	Failure Mode & Crack Severity	Panel Crack Width (mm)	State	IDR
DS1	Small crack	Figure 10a	0.01	First yield	0.17%
DS2	Diagonal cracks are starting to connect, block damage in panels	Figure 10b	0.22	Elastic–Plastic	0.52%
DS3	Cross-shaped cracks and block damage to panels increases	Figure 10c	0.69	Ultimate	0.79%
DS4	Failed/collapse	Figure 10d	1.91	Collapse	1.99%

**Figure 11.** Damage states infilled frame based on the proposed IDR initiated through the local damage panel.

Compared with several references and codes (Table 1), the range of damage states proposed in this study shows little difference. The difference might be due to the complexity of the factors that affect the behavior of the infilled frame, such as the different properties of the constituent materials, the technical brick-making, infilled construction techniques and many others. Especially for the constituent material factors of this infilled frame, a parametric study will be attempted. This method is used to find out in more detail the relationship between the properties of the constituent materials and the behavior of the structure associated with a particular definition of damage. In addition, this method is expected to inform the properties of the constituent materials, which significantly affect the behavior of the infilled frame. Five were chosen for the variable mechanical properties of the infilled frame, considering that these five values are some of the mechanical properties that significantly affect the behavior of the infilled frame. The mechanical properties values that will be used as variations in this numerical model are the compressive strength of concrete ( $f_c$ ), the yield strength of the reinforcement ( $f_y$ ), the reinforcement ratio ( $\rho$ ), compressive strength of masonry ( $F_m$ ) and elasticity modulus of masonry ( $E_m$ ). This variation in mechanical properties is related to the structure's behavior, i.e., in classifying the level of damage, according to the suggestions in this study (Table 8). Through a parametric study using this meso model, the stages of classifying damage states start from investigating the damage/severity of the panels per step and then proceed to define the exact crack width value. After the local damage values are obtained, they are connected to IDR per level of damage states.

In general, Figures 12–16 section (a) shows the relationship between the influence of several variations of the mechanical properties of the infilled frame on the level of damage grouped according to the identification of the proposed crack width (Table 8). Meanwhile, Figures 12–16 section (b) shows the results of grouping the level of structural damage through the initial data (local damage) and then associating it with the IDR value. The recapitulation of Figures 12–16 illustrates that the difference in mechanical properties will result in a different IDR even though the crack width per level of damage has been following the proposed value. This phenomenon is clearly seen when the damage level is DS2, DS3 and DS4. Therefore, the classification of infilled frame damage is highly dependent on complex structural behavior, one of which is the mechanical properties of the constituent materials.

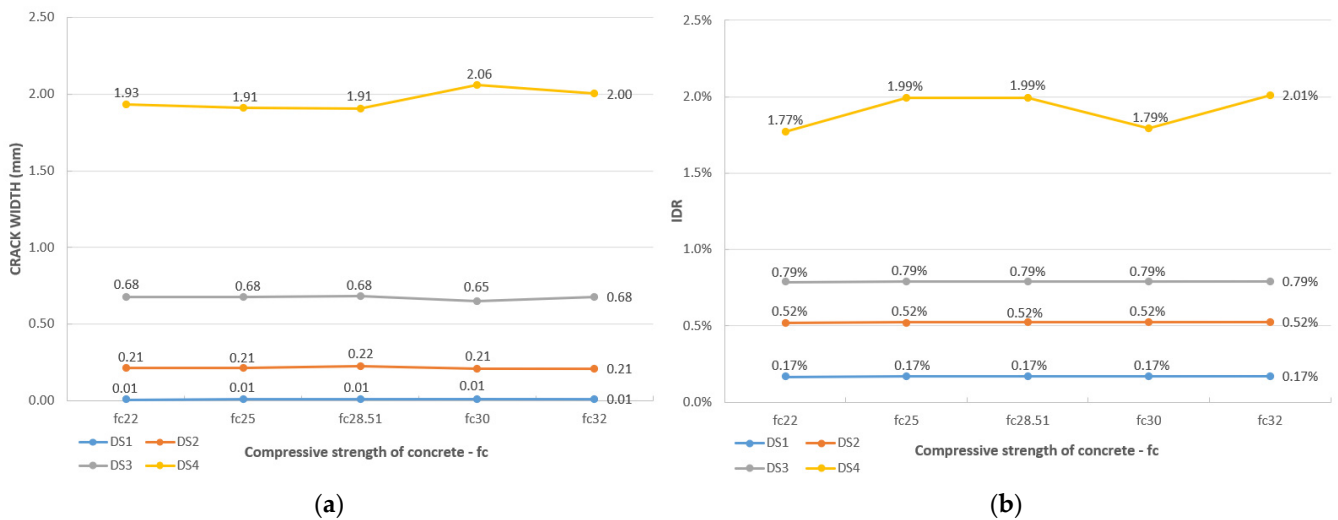


Figure 12. Correlation of damage states (DS) with compressive strength of concrete ( $f_c$ ) associated with: (a) crack width (mm); (b) IDR (%).

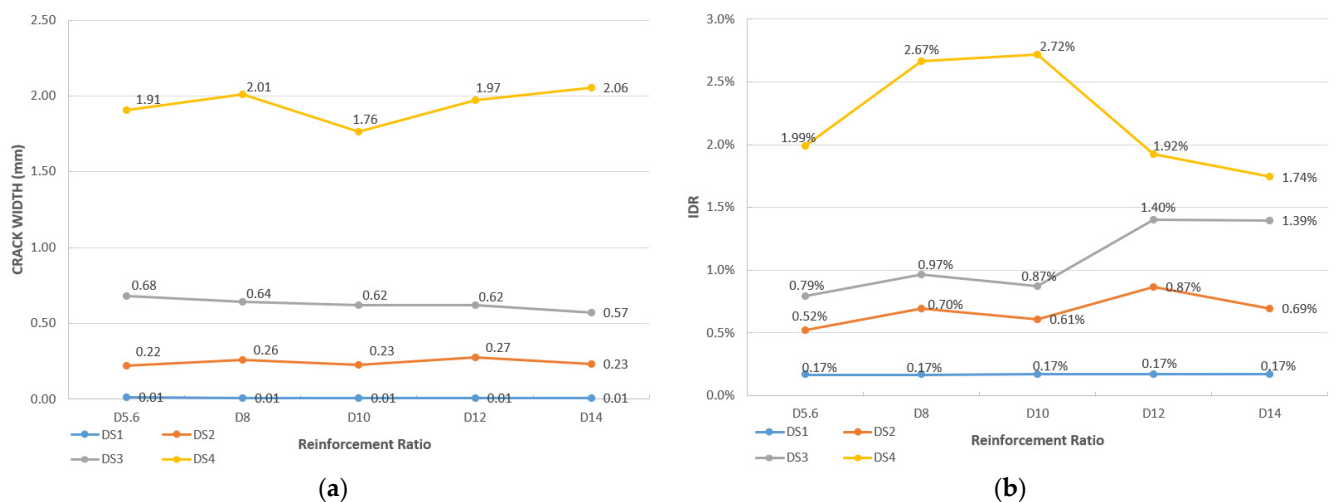
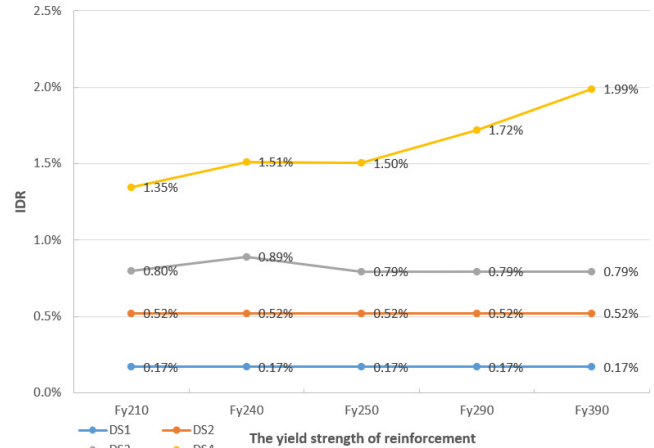
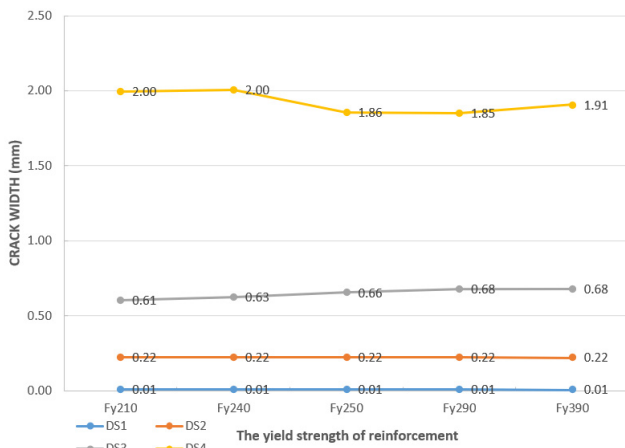


Figure 13. Correlation of damage states (DS) and the ratio of reinforcement ( $\rho$ ) associated with: (a) crack width (mm); (b) IDR (%).

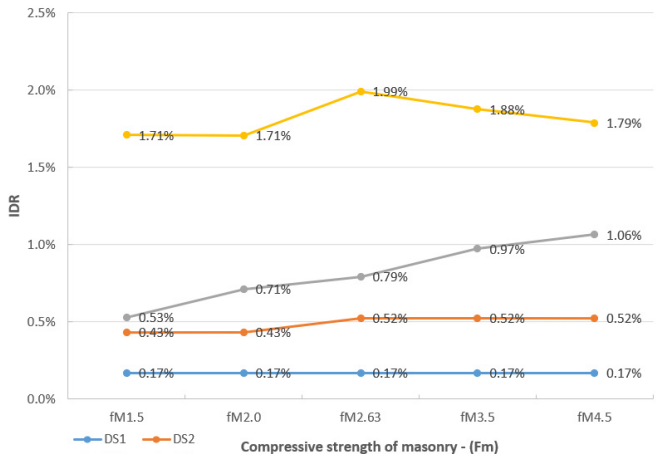
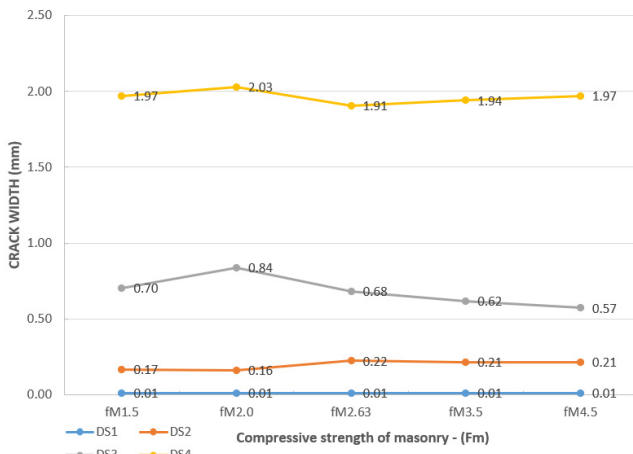




(a)

(b)

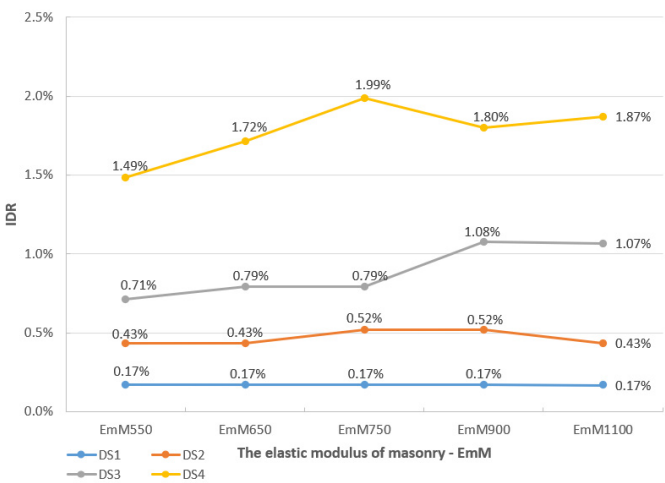
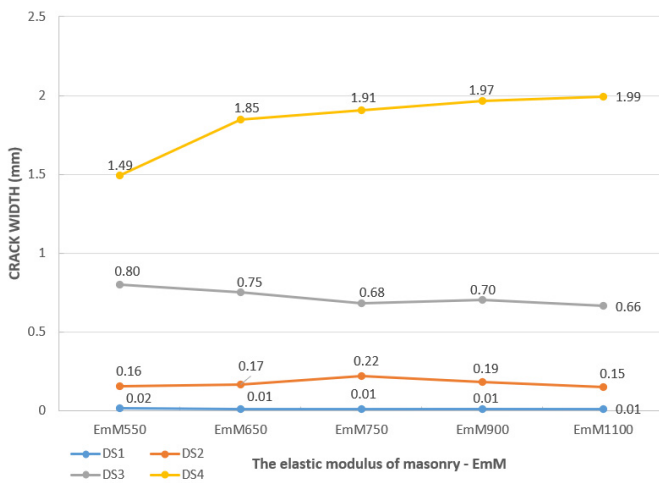
Figure 14. Correlation of damage states (DS) and yield strength of reinforcement ( $f_y$ ) associated with: (a) crack width (mm); (b) IDR (%).



(a)

(b)

Figure 15. Correlation of damage states (DS) and the compressive strength of masonry ( $F_m$ ) associated with: (a) crack width (mm); (b) IDR (%).



(a)

(b)

Figure 16. Correlation of damage states (DS) and elasticity modulus of masonry ( $E_{mM}$ ) associated with: (a) crack width (mm); (b) IDR (%).

It seems that the mechanical properties do not influence the DS1 value. For example, the IDR value of DS1 is 0.17%, regardless of variation in mechanical properties, as shown in Figures 12b, 13b, 14b, 15b and 16b. The minor structural damage at this initial level (DS1) may be the reason. On the contrary, it shows that mechanical properties affect the value of IDR at a high damage state. The higher the damage state, the more significant the effect of the mechanical properties. At a higher damage state, the structure is in an inelastic condition, causing nonlinearity in the behavior of the structure. Subsequently, at severe damage states, i.e., DS3 and DS4, the curve's trend is volatile as the value of mechanical properties increases (see Figures 12b, 13b, 14b, 15b and 16b).

Both models with variations in concrete compressive strength,  $f_c$  (Figure 12b), and the yield strength of the reinforcement,  $f_y$  (Figure 14b), produce the same DS1, DS2, and DS3 values. Based on this data, it can be concluded that concrete compressive strength ( $f_c$ ) and the yield strength of the reinforcement ( $f_y$ ) hardly affect the behavior of the infill wall structure when the condition is still within an elastic–plastic–peak load. Another thing that needs to be observed is the model's output with variations in the yield strength of the reinforcement ( $f_y$ ), shown in Figure 14b. The DS4 value in this variation model shows an upward trend with the increase in the quality of the reinforcement used. Based on this background, it can be concluded that, with the increase in the quality of the reinforcement used, the collapse resistance of the infill wall structure is getting better.

In general, it can be concluded that the numerical method using the meso model is quite effective in determining infilled frame damage conditions based on local damage, which is then linked to global behavior. The local damage is identified based on the failure mode, the severity of the damage and the crack width that occurs on the panel. Meanwhile, global behavior is related to the IDR value. Global damage associated with IDR is needed to simplify the mechanism for classifying damage conditions in infilled frames.

## 7. Conclusions

Numerical modeling is one of the methods used in describing the actual structure model, which can capture the behavior of the structure both when it is elastic and inelastic. The huge benefit that can be taken from the construction of numerical models and their analysis is the ability to perform structural assessments quickly and effectively without compromising the accuracy of the results. This study describes in detail the manufacture of a numerical model to investigate the behavior of elastic-inelastic infilled frames using the meso model. Some important things that can be summarized as the basis for further research development:

- a. The meso model is capable of capturing local damage information on each structural component, including wall panels, which can then be used for determining the level of structural damage.
- b. The stages of grouping the damage states in this study are based on the local damage that occurs in the panel, i.e., the shape of the crack, the severity of the crack and the width of the crack. Local damage per level is associated with the value of the inter-story drift ratio (IDR).
- c. The proposed IDR-based damage state values for infilled frames in this study are DS1 = 0.17%, DS2 = 0.52%, DS3 = 0.79% and DS4 = 1.99%.
- d. The difference in IDR values for each level of damage in several previous studies and this study is due to the complexity of the infilled frame behavior accompanied by different typologies. This is proven through a parametric study conducted in this study using several mechanical properties of infilled frames, i.e., compressive strength of concrete, ratio of reinforcement, yield strength of reinforcement, compressive strength of masonry and elasticity modulus of masonry.
- e. When the structure is still in elastic condition, the difference in mechanical property values does not affect the level of damage to the initial structure—minor (DS1). On the other hand, differences in the values of mechanical properties cause the values of DS2, DS3 and DS4 to have fluctuate differences. This is due to the degree of damage

occurring when the structure is in an after-elastic condition, so this inelastic condition results in nonlinear behavior of the structure.

## 8. Recommendation

In general, it can be concluded that when assessing the performance requirements of simple infill structures, the meso model approach can be used. However, if the infilled frame has a variety of elemental complexity, then infilled frame modeling through a finite element micro model approach is highly recommended.

**Author Contributions:** I.R.H. performed numerical simulation, analyzed data, and wrote the initial draft of the manuscript; S.A.K. contributed to the original conception, supervised the work, and reviewed the draft; B.S.G. supervised the work and reviewed the draft; S.S. supervised the work, and reviewed the draft. All authors have read and agreed to the published version of the manuscript.

**Funding:** This research was funded by the Ministry of Education, Culture, Research and Technology of Indonesia, SK number 033/E5/PG.02.00/2022 and Contract Number 096/E5/PG.02.00.PT/2022 & 673.1/UN27.22/PT.01.03/2022.

**Institutional Review Board Statement:** Not applicable.

**Informed Consent Statement:** Not applicable.

**Data Availability Statement:** The data presented in this study is available on request from the corresponding author.

**Conflicts of Interest:** The authors declare no conflict of interest.

## References

1. Khan, N.A.; Monti, G.; Nuti, C.; Vailati, M. Effects of Infills in the Seismic Performance of an RC Factory Building in Pakistan. *Buildings* **2021**, *11*, 276. [[CrossRef](#)]
2. Zhang, B. Parametric Study on the Influence of Infills on the Displacement Capacity of RC Frames for Earthquake Loss Estimation. Master's Thesis, Rose School, Pavia, Italy, 2006.
3. Furtado, A.; Rodrigues, H.; Arède, A.; Varum, H. Experimental Characterization of the In-plane and Out-of-Plane Behaviour of Infill Masonry Walls. *Procedia Eng.* **2015**, *114*, 862–869. [[CrossRef](#)]
4. Hapsari, I.R.; Sangadji, S.; Kristiawan, S.A. Seismic performance of four-storey masonry infilled reinforced concrete frame building. In *MATEC Web of Conferences*; EDP Sciences: Les Ulis, France, 2018; Volume 195, p. 02017. [[CrossRef](#)]
5. Vahidi, E.K.; Malekabadi, M.M. Conceptual investigation of shortcolumns and masonry infill frames effect in the earthquakes. *Int. J. Civ.* **2009**, *3*, 472–477.
6. Rodrigues, H.; Varum, H.; Costa, A. Simplified Macro-Model for Infill Masonry Panels. *J. Earthq. Eng.* **2010**, *14*, 390–416. [[CrossRef](#)]
7. Butenweg, C.; Marinković, M.; Salatić, R. Experimental results of reinforced concrete frames with masonry infills under combined quasi-static in-plane and out-of-plane seismic loading. *Bull. Earthq. Eng.* **2019**, *17*, 3397–3422. [[CrossRef](#)]
8. D'Aragona, M.G.; Polese, M.; Di Ludovico, M.; Prota, A. Seismic Vulnerability for RC Infilled Frames: Simplified Evaluation for As-Built and Retrofitted Building Typologies. *Buildings* **2018**, *8*, 137. [[CrossRef](#)]
9. Furtado, A.; Teresa de Risi, M. Recent Findings and Open Issues concerning the Seismic Behaviour of Masonry Infill Walls in RC Buildings. *Adv. Civ. Eng.* **2020**, *2020*, 9261716. [[CrossRef](#)]
10. Nucera, F.; Santini, A.; Tripodi, E.; Cannizzaro, F.; Pantò, B. Influence of geometrical and mechanical parameters on the seismic vulnerability assessment of confined masonry buildings by macro-element modeling. In *Proceedings of the 15th World Conference on Earthquake Engineering*, Lisbon, Portugal, 24–28 September 2012; pp. 24–28.
11. Stoica, D. About Masonry Walls Ductility Capacities Calculation. In *Proceedings of the 3rd International Conference Research & Innovation in Engineering*, Brasov, Romania, 16–17 October 2014; pp. 173–178.
12. Crisafulli, F.J. Seismic Behaviour of Reinforced Concrete Structures with Masonry Infills. Ph.D. Thesis, University of Canterbury, Christchurch, New Zealand, 1997.
13. IMeli, R.; Alcocer, S.M.; Leon, F.; Sanchez, T.A. Experimental study on earthquake-resistant design of confined masonry structures. *Earthq. Eng.* **1992**, *6*, 3469–3474.
14. Flores, L.E.; Alcocer, S.M. Calculated response of confined masonry structures. In *Proceedings of the 11th World Conference on Earthquake Engineering*, Acapulco, Mexico, 23–28 June 1996; pp. 1–8.
15. Varela-Rivera, J.; Fernandez-Baqueiro, L.; Alcocer-Canche, R.; Ricalde-Jimenez, J.; Chim-May, R. Shear and Flexural Behavior of Autoclaved Aerated Concrete Confined Masonry Walls. *ACI Struct. J.* **2018**, *115*, 1453–1462. [[CrossRef](#)]

16. Flores, L.E.; Alcocer, S.M. Displacement Capacity of Confined Masonry Structures Reinforced with Horizontal Reinforcement: Shaking Table Tests. In Proceedings of the 16th World Conference on Earthquake Engineering, Santiago, Chile, 9–13 January 2017; pp. 1–12.
17. Quiroz, L.G.; Maruyama, Y.; Zavala, C. Cyclic behavior of Peruvian confined masonry walls and calibration of numerical model using genetic algorithms. *Eng. Struct.* **2014**, *75*, 561–576. [[CrossRef](#)]
18. Tena-Colunga, A.; Juárez-Ángeles, A.; Salinas-Vallejo, V.H. Cyclic behavior of combined and confined masonry walls. *Eng. Struct.* **2009**, *31*, 240–259. [[CrossRef](#)]
19. Akhaveissy, A.H.; Abbassi, M. Pushover analysis of unreinforced masonry structures by fiber finite element method. *Res. Civ. Environ. Eng.* **2014**, *2*, 96–119.
20. Lourenco, P.B. Computational Strategies for Masonry Structures. Ph.D. Thesis, Delft University of Technology, Delft, The Netherlands, 1996.
21. Asteris, P.G.; Antoniou, S.T.; Sophianopoulos, D.S.; Chrysostomou, C.Z. Mathematical Macromodeling of Infilled Frames: State of the Art. *Eng. Struct.* **2011**, *137*, 1508–1517. [[CrossRef](#)]
22. Van der Mersch, W. Modelling the Seismic Response of an Unreinforced Masonry Structure. Master's Thesis, Delft University of Technology, Delft, The Netherlands, 2015.
23. Baker, J.W. Measuring bias in structural response caused by ground motion scaling. In Proceedings of the 8th Pacific Conference on Earthquake Engineering, Singapore, 5–7 December 2007; pp. 1–8.
24. Ghobarah, A. Performance-based design in earthquake engineering: State of development. *Eng. Struct.* **2001**, *23*, 878–884. [[CrossRef](#)]
25. Arumugam, V.; Keshav, L.; Achuthan, A.; Dasappa, S. Seismic Evaluation of Advanced Reinforced Concrete Structures. *Adv. Mater. Sci. Eng.* **2022**, *2022*, 4518848. [[CrossRef](#)]
26. Colangelo, F. Drift-sensitive non-structural damage to masonry-infilled reinforced concrete frames designed to Eurocode 8. *Bull. Earthq. Eng.* **2013**, *11*, 2151–2176. [[CrossRef](#)]
27. Cardone, D.; Perrone, G. Developing fragility curves and loss functions for masonry infill walls. *Earthquakes Struct.* **2015**, *9*, 257–279. [[CrossRef](#)]
28. Chiozzi, A.; Miranda, E. Fragility functions for masonry infill walls with in-plane loading. *Earthq. Eng. Struct. Dyn.* **2017**, *46*, 2831–2850. [[CrossRef](#)]
29. Stavridis, A. Analytical and Experimental Study of Seismic Performance of Reinforced Concrete Frames Infilled with Masonry Walls. Ph.D. Thesis, University of California, San Diego, CA, USA, 2009.
30. Page, A.W. Finite Element Model for Masonry. *J. Struct. Div.* **1978**, *104*, 1267–1285. [[CrossRef](#)]
31. Polyakov, S.V. *Masonry in Framed Buildings. Gosudalst-Vennoe'stvo Literature po Straitel' stuv i Arkitecture, Moscow, Russia*; Cairns, G.L., Translator; Building Research Station: Watford, UK, 1956.
32. Crisafulli, F.J.; Carr, A.J. Proposed macro-model for the analysis of infilled frame structures. *Bull. N. Z. Soc. Earthq. Eng.* **2007**, *40*, 69–77. [[CrossRef](#)]
33. Chrysostomou, C.; Gergely, P.; Abel, J.F. A Six-Strut Model For Nonlinear Dynamic Analysis Of Steel Infilled Frames. *Int. J. Struct. Stab. Dyn.* **2002**, *2*, 335–353. [[CrossRef](#)]
34. Kumar, M.; Khalid, F.; Ahmad, N. Macro-Modelling of Reinforced Concrete Frame Infilled with Weak Masonry for Seismic Action. *NED Univ. J. Res.* **2018**, *15*, 15–38.
35. Elgaaly, M.; Hamid, A.A. Three-Strut Model for Concrete Masonry-Infilled Steel Frames. *Eng. Struct.* **2003**, *129*, 177–185. [[CrossRef](#)]
36. Tanganelli, M.; Rotunno, T.; Viti, S. On the modelling of infilled RC frames through strut models. *Cogent Eng.* **2017**, *4*, 1371578. [[CrossRef](#)]
37. Pashaie, M.R.; Mohammadi, M. Estimating the local and global effects of infills on steel frames by an improved macro-model. *Eng. Struct.* **2019**, *187*, 120–132. [[CrossRef](#)]
38. SEAOC. *Vision 2000-A Framework for Performance Based Earthquake Engineering*; Structural Engineers Association of California; Seismology Committee: Sacramento, CA, USA, 1995.
39. Applied Technology Council. *ATC-40 Seismic Evaluation and Retrofit of Concrete Buildings*; Applied Technology Council: Redwood City, CA, USA, 1996; Volume 1.
40. FEMA. *NEHRP Guidelines for the Seismic Rehabilitation of Buildings*; FEMA 273: Washington, DC, USA, 1996.
41. Liu, C.; Liu, B.; Wang, X.; Kong, J.; Gao, Y. Seismic Performance Target and Fragility of Masonry Infilled RC Frames under In-Plane Loading. *Buildings* **2022**, *12*, 1175. [[CrossRef](#)]
42. Šipoš, T.K.; Hadzima-Nyarko, M.; Miličević, I.; Grubišić, M. Structural Performance Levels for Masonry Infilled Frames. In Proceedings of the 16th European Conference on Earthquake Engineering, Thessaloniki, Greece, 18–21 June 2018; pp. 1–12.
43. Krawinkler, H. A few basic concepts for performance based seismic design. In Proceedings of the 11th World Conference on Earthquake Engineering, Acapulco, Mexico, 23–28 June 1996; Volume 1133.
44. Zhang, M.Y. Components Performance-Based Seismic Vulnerability Analysis of Masonry infilled Frame Structures. Master's Thesis, Institute of Engineering Mechanics, China Earthquake Administration, Harbin, China, 2017.
45. Kakaletsis, D.J.; Karayannis, C.G. Experimental Investigation of Infilled Reinforced Concrete Frames with Openings. *ACI Struct. J.* **2009**, *106-S14*, 132–141.

46. Beer, M.; Kougoumtzoglou, I.A.; Patelli, E.; Au, I.S.-K. *Encyclopedia of Earthquake Engineering*; Springer: Berlin/Heidelberg, Germany, 2015. [[CrossRef](#)]
47. Cervenka, V.; Jendele, L.; Cervenka, J. *ATENA Program Documentation Part 1 Theory*; Cervenka Consulting Ltd.: Prague, Czech Republic, 2012.
48. Cervenka, V.; Cervenka, J.; Pukl, R. ATENA—A tool for engineering analysis of fracture in concrete. *Sadhana* **2002**, *27*, 485–492. [[CrossRef](#)]
49. Sato, R.; Sogo, S.; Kanazu, T.; Kishi, T.; Noguchi, T.; Mizobuchi, T.; Miyazawa, S. JCI guidelines for control of cracking of mass concrete 2008. *Sustain. Constr. Mater. Technol.* **2013**, *1*, 18–21.
50. *ACI 318-19; Building Code Requirements for Structural Concrete (ACI 318R-19) and Commentary (ACI 318R-19)*. ACI: Farmington Hills, MI, USA, 2019. [[CrossRef](#)]
51. Vonk, R.A. Softening of Concrete Loaded in Compression. Ph.D. Thesis, Technische Universiteit Eindhoven, Eindhoven, The Netherlands, 1992.
52. Van Mier, J.B.M. Strain-Softening of Concrete under Multiaxial Loading Conditions. Ph.D. Thesis, Technische Hogeschool Eindhoven, Eindhoven, The Netherlands, 1984.
53. Prasad, M.D.R.; Shakeeb, S.; Chandradhara, G.P. Nonlinear behavior of Reinforced Concrete Infilled Frames using ATENA 2D. *Indian J. Adv. Chem. Sci.* **2016**, *1*, 173–178.
54. Ahmed, A.; Shahzada, K. Seismic vulnerability assessment of confined masonry structures by macro-modeling approach. *Structures* **2020**, *27*, 639–649. [[CrossRef](#)]
55. Anić, F.; Penava, D.; Guljaš, I.; Sarhosis, V.; Abrahamczyk, L.; Butenweg, C. The Effect of Openings on Out-of-Plane Capacity of Masonry Infilled Reinforced Concrete Frames. In Proceedings of the 16th European Conference on Earthquake Engineering, Thessaloniki, Greece, 18–21 June 2018; pp. 1–11.

**Disclaimer/Publisher’s Note:** The statements, opinions and data contained in all publications are solely those of the individual author(s) and contributor(s) and not of MDPI and/or the editor(s). MDPI and/or the editor(s) disclaim responsibility for any injury to people or property resulting from any ideas, methods, instructions or products referred to in the content.